Sensors and Actuators A 192 (2013) 58–68

Contents lists available at SciVerse ScienceDirect

Sensors and Actuators A: Physical

journal homepage: www.elsevier.com/locate/sna

The effect of periodic magnetic force on a piezoelectric energy harvester

Yunus Uzun [a,*], Erol Kurt [b]

[a] Department of Electrics and Energy, Vocational School, Ahi Evran University, 40100 Kirsehir, Turkey
[b] Department of Electrical and Electronics Engineering, Faculty of Technology, Gazi University, 06500 Teknikokullar, Ankara, Turkey

ARTICLE INFO

Article history:
Received 22 February 2012
Received in revised form
14 December 2012
Accepted 14 December 2012
Available online 21 December 2012

Keywords:
Energy harvester
Softening nonlinearity
Periodic magnetic force
Piezoelectric beam

ABSTRACT

The response of a piezoelectric (PZT) harvester in pendulum shape is explored under a periodic magnetic field both theoretically and experimentally. The magnetic force F_m is found via fitting to a polynomial function including the third order of amplitude after the evaluation of magnetic simulations. F_m term dominates the dynamics of the piezoelectric (PZT) harvester with a certain frequency ω_m and the excitation amplitude U_m. A clear softening effect is observed as function of excitation frequency. Besides, the output power estimation is in good agreement with the experimental results. While the amplitude changes sinusoidal, velocity of the pendulum tip especially includes a number of different high frequency components with growing amplitudes. The periodic excitation causes ripples at the maximal and minimal values of velocity. Excitation frequency ω_m, which differs from the natural frequency ω_0 causes much complex velocity data with high frequency components. The averaged power $P = 79\ \mu W$ can be obtained and power increases dramatically when the harvester is excited at the natural frequency.

1. Introduction

Energy harvesting studies have been of great interest for the development of autonomous sensor nodes and microsystems in order to achieve better lifetimes for the regenerative systems and operations [1,2]. Portable and wireless devices such as low power computing, sensors and communications can have longer battery life, thereby less recharging time by introducing different harvesting mechanisms, if above-mentioned devices or systems are supported by an energy harvester. Among the harvesting mechanisms, the conversion of mechanical energy from background vibrations into electrical energy via a piezoelectric (PZT) converter is the most common one [1–4]. According to literature, a PZT harvester can be much effective, if it is operated at resonance frequency [5,6]. In fact, the harvested energy considerably decays in frequency-varying harvesting systems and wide-band vibrations are observed as results of random excitations in nature. Thus, most of the background vibrations lead to wide frequency spectra as a result of random natural strengths. Therefore, the exploration of harvesters in terms of their dynamic responses under different excitation frequencies and amplitudes are important goals in order to harvest much energy from the magnetic ambient. As one of the excitation type-external magnetic excitation on such harvesters have been explored recently in order to increase the efficiency of different harvester systems in terms of wide-band vibrations [1,7,8]. Many different designs under various magnetic excitation types have been reported in the literature [1,7–9]. For instance, a harvester including four permanent magnets in a homogeneously exerted magnetic field was designed and implemented as an inverted pendulum in a recent work by Cottone et al. [7]. They have explored some dynamical features of stochastically nonlinear vibrations and generated an energy output by using an external stable magnetic media. Since they used many permanent magnets and a stable magnetic field excitation, their system requires a large space for installation in advance. In one of the recent papers, Ferrari et al. [1] have proven that the wideband vibrations which are resulted by the permanent magnets can improve the output power upto 250% in magnetical-excited piezoelectric layers. Therefore we motivate ourselves in order to explore the responses at varying excitation schemes. On the other hand, in terms of nonlinearity, the bistable systems which have two equilibrium positions give better energy harvesting mechanism. Such systems can be implemented by either considering only the mechanical aspects of the systems or introducing an external nonlinear force [10]. Such a bistability enables the system to switch between two stable states, namely bistable and monostable states by increasing the velocity and power converted by the harvester. The analytical background on this mechanism was studied Ramlan et al. and Stanton et al. [9,11]. However we proposed another nonlinear effect for the vibration of a beam by introducing nonautonomous (i.e. time-dependent) magnetic field in the earlier papers [12,13]. The complicated responses of a magnetoelastic beam in a time-varying magnetic field without the PZT layer were examined experimentally and theoretically. A large variety of dynamic responses such

* Corresponding author. Tel.: +90 386 211 47 24; fax: +90 386 211 47 51.
E-mail addresses: yuzun@ahievran.edu.tr (Y. Uzun), ekurt@gazi.edu.tr (E. Kurt).

0924-4247/$ – see front matter © 2012 Elsevier B.V. All rights reserved.
http://dx.doi.org/10.1016/j.sna.2012.12.017

as periodic and chaotic amplitudes were observed and bistable modes were also observed for certain parameters. We proved that the damping coefficient γ played an important role to characterize such vibration systems. Besides, the effects of field excitation frequencies in terms of even and odd values are undeniable in the sense that the system becomes much complex for odd field frequencies (see in [12]). The intermediate regimes of two-well chaos (i.e. bistable mode) were also survived for the appropriate parameter sets in order to determine the large amplitude oscillations, which yield to higher energy outputs. Since the transition from one well to two well chaos (i.e. a transition to the bistable potential mode) causes larger displacements, the amount of the obtained energy can be increased further as also pointed out by Ferrari et al. [1]. Similar analyzes indicate that the nonlinear systems can generate large-amplitude oscillations over a wider frequency range with respect to the linear case [14,15], thus one can harvest higher energies under proper conditions. However, according to above studies, the authors have used permanent magnets and mechanical excitations in their setups, therefore the effects of periodic magnetic excitation are still incomplete and the harvesting features (i.e. output power, load, field frequency, the distance to magnetic source) under periodic field have not been fully explored yet.

There exists various energy harvesting systems which can be applied under a magnetic environment. Among them, electromagnetic and electrostatic systems are alternative to the magneto-piezoelectric systems. However energy density of piezoelectric systems under magnetic media can lead to higher energy densities such as 35 mJ/cm^3 compared to the pure electromagnetic or electrostatic systems [16]. In addition, piezoelectric systems can generate higher voltages upto 10 V compared to the electromagnetic energy converting systems [17]. Therefore piezoelectric harvesters are much promising due to above-mentioned reasons. On the other hand, piezo-harvesters can be configured as a compact system and therefore it can be much suitable for microelectromechanical systems (MEMS) [17].

In the present paper, we report the effects of periodic field excitation for the harvester in order to make a feasibility study on the energy harvesting mechanism under periodic magnetic field. The proposed harvester can be easily adapted to any working device such as generators, relays and motors which exert a changeable magnetic media as our preliminary studies have been recently reported in [18]. According to the experimental results, this piezoelectric pendulum can harvest power of 3.5 μW, if nearly 1.3 A current flows from a winding in a 3-phase induction motor under no mechanical load. From the experimental point of view, such a current can exert 4 G flux density out of the motor according to our measurements by FW-Bell 5170 gaussmeter. In a recent study, Borin et al. have also observed a certain leakage flux density out of the motor [19]. It will be stated later that the nonlinear nature of the magnetic force as function of displacement and current yields to different responses of the piezoelastic beam tip. The displacement and velocity of beam tip, harvested voltage over the load and output power of the harvester are explored as function of different external magnetic stress. In addition, a theoretical modeling and power estimation have been clarified in order to complete the relation between the experiment and theory. Thus the parametrical dependences of the piezoelastic beam are governed by the partial differential equations in space and time theoretically.

2. Experimental description of the harvester

The experimental setup for the exploration of piezoelectic harvester response is sketched in Fig. 1(a). The displacement of the beam tip caused by the electromagnet is elaborated in Fig. 1(b) with the appropriate variables. The overall setup mainly consists of six

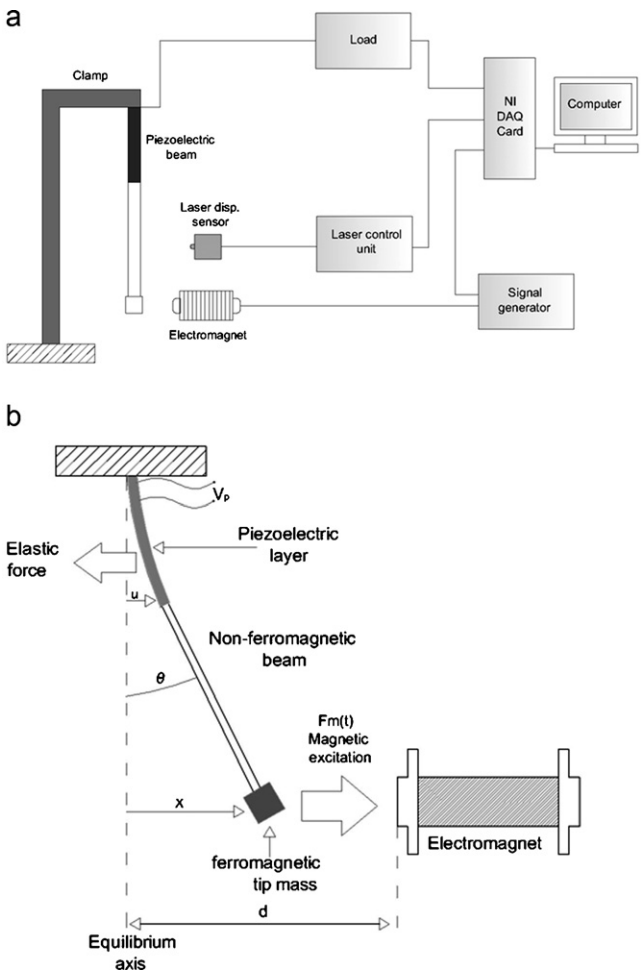

Fig. 1. (a) A schematic representation of the piezoelectric energy harvesting system. (b) Forces acting on the piezoelectric energy harvester near the electromagnet.

units: The magnetic excitation unit, non-ferromagnetic beam with piezoelectric thin layer (Lead zirconate titanate, i.e. PZT), laser displacement sensor (LDS), signal generator, and data acquisition and monitoring unit. The system arranged as a pendulum including a ferromagnetic tip mass (having 1 cm × 1 cm × 1 cm size) at the tip of the pendulum. The piezoelastic layer has been positioned at the top of the pendulum connecting the non-ferromagnetic beam to the clamp.

The external magnetic force is exerted to the pendulum, so that an oscillation starts at the beam, thus a measurable voltage signal is generated at the output of PZT material. In principle, the oscillation is mainly characterized by the external varying magnetic force, elastic force and the damping effects in the system. While a finite magnetic force acts on the tip in an increasing trend for half period, that opposes the elastic restoring force of the bended beam. In the decreasing part of magnetic force at the rest of the period, the elastic restoring forces dominate the system mostly. Fig. 1(b) shows the displacement of the beam tip at an instant time. The laser displacement sensor (LDS) measures the displacement of the tip mass with a high accuracy during the operation, thereby the tip velocity can be determined by evaluating the position data at exact time. Both the input of magnetic excitation unit and the generated signal can be controlled and observed via a computer. Since the amplitude and the frequency of the applied signal to the electromagnet can be adjusted, the motion can be controlled and a wide range of parameter space can be scanned. Then, voltage generated by the piezoelastic layer is used to drive the load R_L.

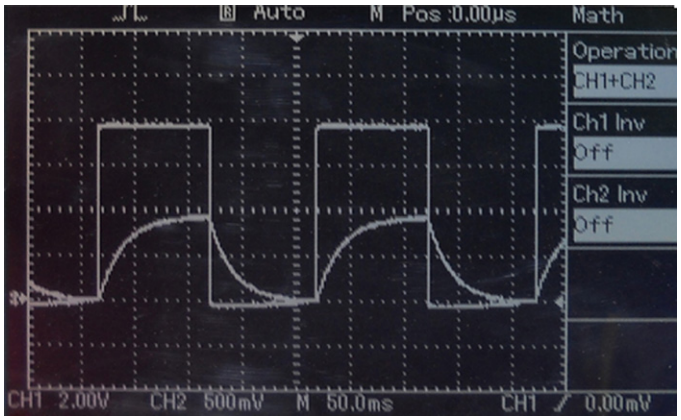

Fig. 2. The square voltage V_c applied to the electromagnet and the current I_c flowing inside the coil of electromagnet for magnetic excitation at a certain frequency ω_m.

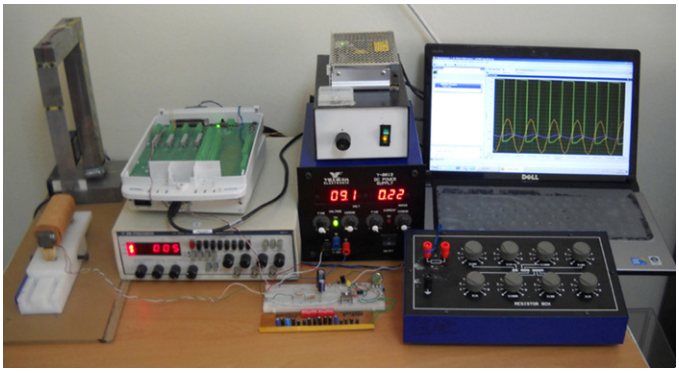

Fig. 3. Experimental setup: from left to right, piezoelectric layer with non-ferromagnetic beam, laser displacement sensor (LDS), electromagnet, DAQ card, signal generator, electromagnet and LDS feeding sources, laptop and variable resistive load.

During the entire period of the motion, damping effects are also observable. Basically, the elastic restoring forces of the beam and piezoelastic layer compete with the external magnetic force in that sense. Since the voltage over the electromagnet has a step-pulsed character, magnetic excitation unit applies a varying flux on the tip mass. The square wave of the excitation voltage which is applied to the electromagnet and its response are shown in Fig. 2. Since the magnetic force is characterized by the current flowing the electromagnet, the current wave form generated by the electromagnet is shown as growing and decaying exponential functions (Eq. (5)) for each period (Fig. 2). The magnetic periodic force is characterized as function of current I_c and the position of the piezoelectric layer tip u.

In the experiments, a PZT layer having the sizes of 70 mm × 32 mm × 1.5 mm and the weight of 10 g and produced by Piezo System Inc. was used. The capacitance and stiffness values of PZT layer are 232 nF and 188 N/m, respectively. The aluminum non-ferromagnetic beam has dimensions of 135 mm × 30 mm × 1.5 mm with Young's module of 70 GPa. The non-magnetic beam has been attached to PZT layer via two small screws firmly. The laser displacement sensor (LDS) has a head with type IL-065 and a control unit IL-1000 made by Keyence Inc. A step-pulsed signal generating circuit, and an NI USB-6250 data acquisition unit are also used in the setup. The magnetic excitation unit includes an electromagnet having 1050 turns with 0.70 diameter copper wire. The ferromagnetic core has the dimension of 120 mm × 20 mm × 20 mm and a relative permeability of μ_r = 10,000. A step-pulsed voltage with certain amplitude U_{max} and frequency ω_m is applied to the coil in order to exert a certain magnetic stress at the tip of harvester. The laser displacement sensor which measures the displacement of the beam tip has a sufficient sensitivity of 4 μm. This laser displacement sensor head can measure the vibrations with the sampling rate of 1 ms. The data acquisition card has 16 analog inputs, thereby it is possible to get multiple records of different physical parameters such as displacement, and input/output voltages in the experiments, synchronously. The overall setup is shown in Fig. 3.

More than 500,000 data points can be captured per second by this card. For data treatment and documentation, we collect all experimental outputs into *LabVIEW* software. In order to determine the responses of harvester at different distances d to electromagnet, an adjustable slide mechanism which is connected to the bottom of electromagnet is used. Therefore the electromagnet can be moved forward and backward with respect to the harvester in order to adjust new distance d for measurements. Input voltages to the electromagnet are adjusted between 6 V and 10 V during the experiments according to the exploration of the system parameters in order to increase the magnetic force F_m.

Fig. 4 represents the measurement of the pure output signal which is generated from the PZT layer. The voltage measurements were realized over different resistive loads R_L between 10 kΩ and 10 MΩ, experimentally.

3. Theoretical background

The theoretical background of the piezoelectric energy harvester in a changeable magnetic media is defined at this section. In one of our earlier paper, some mechanical features of such an elastic beam were described (see [13]). In the present study, an external magnetic field obtained by an electromagnet affects a ferromagnetic tip mass attached to a piezoelectric layer (Fig. 1(b)). The varying field is generated near the tip of harvester. In our previous studies, it was found [12,13] that a varying homogeneous field could be created near the tip of an electromagnet and this can drive the tip mass spatio-temporally.

In order to determine the magnetic force $F_m(x,i,t)$, an electromagnet has been designed by the Superfish software which uses the finite element method. In order to explore the force induced on the tip mass, a sufficient number of mesh nodes in horizontal and vertical direction are used. The calculations are realized for a ferrite core. According to the simulations, the flux density decreases at the region between the tip mass and core, however the ferromagnetic tip mass gathers the flux lines on itself homogeneously (Fig. 5). Note that this simulation gives a magnetostatic solution whereas the resulting magnetic force values can be generalized as function of time and winding current inside the coil.

The entire model of a piezoelastic (PZT) pendulum includes the mechanical and electrical aspects. Strictly speaking, Fig. 6 summarizes the entire system as a mass-spring, a damper and a capacitor. Here the rigid mass m_p and the stiffness constant k determine the mechanical structure under a damper γ which gives the mechanical losses.

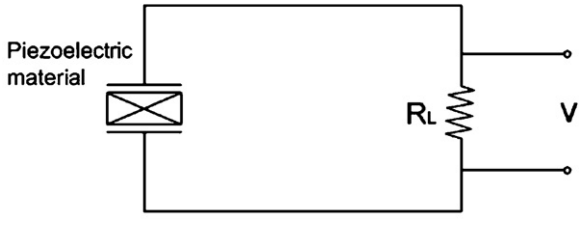

Fig. 4. The output voltage over the load resistance generated by PZT layer.

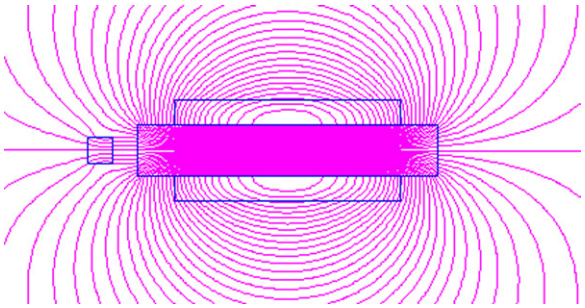

Fig. 5. The tip mass of the beam in front of the electromagnet core. Distance between the tip mass and the core is 1 cm and the current is 1.5 A for this case.

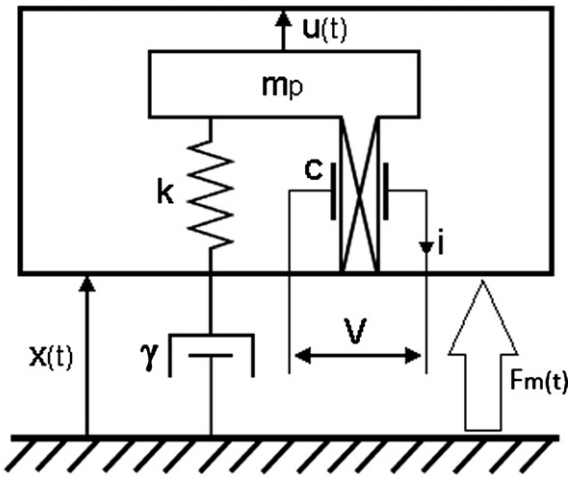

Fig. 6. Equivalent dynamical model of the piezoelectric beam under magnetic excitation.

When a mass displacement u occurs in the PZT, a current i and a voltage V are produced. The relation between the mechanical and electrical units is given by

$$F_{total} = ku + \alpha V + F_m, \quad i = \alpha \frac{du}{dt} - C\frac{dV}{dt}. \tag{1}$$

Here C is the clamped capacitance and α is the force factor. The total equation of motion for the displacement of mass, $u'(t)$ inside the PZT as a result of the pendulum displacement $x'(t)$ can be stated as follows:

$$(m+m_p)\frac{d^2x'}{dt'^2} = -\gamma\frac{du'}{dt'} - m_p\frac{d^2u'}{dt'^2} - ku' - \alpha V - F_m(t), \tag{2}$$

where m denotes the pendulum mass.

While considering the periodic field F_m, the overall dynamic and electrical equations can be stated as follows:

$$\frac{d^2x'}{dt'^2} = -\frac{\gamma}{(m+m_p)}\frac{du'}{dt'} - \frac{m_p}{(m+m_p)}\frac{d^2u'}{dt'^2} - \frac{k}{(m+m_p)}u' - \frac{\alpha}{(m+m_p)}V - \frac{1}{(m+m_p)}F_m(t),$$
$$\frac{dV'}{dt'} = \frac{\alpha}{C}\frac{du'}{dt'} - \frac{i}{C}, \tag{3}$$

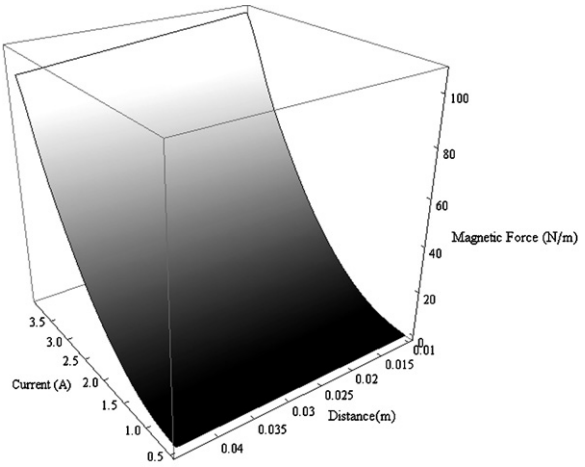

Fig. 7. The magnetic force on the plane of distance and current near the tip of an electromagnet at steady state.

where the mechanical losses are proportional to the velocity of the pendulum. Since the amplitude x proportional to 3 times of the displacement u of piezoelectric layer according to the length ratio, one reads as $u' = 0.33x'$. Therefore the resulting dynamic equation can be simplified as:

$$\frac{d^2u'}{dt'^2} = -\frac{\gamma}{3m+4m_p}\frac{du'}{dt'} - \frac{k}{3m+4m_p}u' - \frac{\alpha}{3m+4m_p}V - \frac{1}{3m+4m_p}F_m(t)$$
$$\frac{dV'}{dt'} = \frac{\alpha}{C}\frac{du'}{dt'} - \frac{i}{C} \tag{4}$$

Eq. (4) can now be used for the mechanical and electrical determination of the system. In our problem, the external magnetic field is obtained by an electromagnet and it is considered to affect a ferromagnetic tip mass attached to the pendulum (Fig. 1). Since the elastic force is much larger than the gravitational one, one can consider the effects of elastic and magnetic forces as in the earlier papers [12,13]. For the determination of the polynomial expression of the magnetic force, a detailed magnetostatic analysis has been carried out following the analysis as in Fig. 5. In that manner, a ferromagnetic body representing the tip mass was initially considered near the electromagnet and the magnetic forces affecting the tip mass were measured in a 2D media for different distances. The resulting function was obtained by the fitted values. According to our model, the periodic excitation force F_m can be considered as follows from the magnetostatic solutions:

$$F_m(t) = \left\{\frac{1-0.7056}{d} + 0.0623(1-3u) + 28026d(1-3u)^2 - 10^6d^2(1-3u)^3\right\}\left\{8\times10^{-8}i_c(t)^2 - 10^{-9}i_c(t)\right\}$$
$$i_c(t) = \begin{cases} \frac{V_c}{R_c}(1-e^{-R_ct/L}) & 0 < t \le \frac{T}{2} \\ \frac{V_c}{R_c}e^{-R_ct/L} & \frac{T}{2} < t \le T \end{cases} \tag{5}$$

Here d, V_c, R_c, L denote the distance from the electromagnet tip to the pendulum equilibrium, the voltage, resistance and inductance of electromagnet coil, respectively. For the simplicity, we consider a purely resistive load directly connected to PZT as in the many other studies [20–22]. We summarize the magnetostatic simulation results in Fig. 7 in order to find out the fitted equation (Eq. (5)) as a periodic magnetic force.

Magnetic force on the plane of distance to the coil tip from the equilibrium point of harvester tip mass and current inside the coil windings is shown in Fig. 7. This graph is produced by using the electromagnetic simulation results. According to this graph, magnetic force decreases smoothly as function of the distance for any constant winding current. However, the effect of winding current is much more important since the force values increase drastically as function of current. For instance, one should keep in mind that the force value falls to 2 N/m for the current value of 2.5 A and the distance value of 1 cm. By following that graph, one can adopt the desired current amount for the excitation of the electromagnet.

In order to obtain the dimensionless form of Eq. (4), we introduce $t' = \tau t$, $y' = yd/\tau$, $u' = ud$ and $V' = V_0 V$ for time, velocity, position and voltage scaling, respectively. Note that τ determines the natural period of the pendulum and cannot be confused by the excitation period of the magnetic field T. In addition, to avoid the misunderstanding, d in later two expressions refers to the distance between the equilibrium point of pendulum and the tip of electromagnet. Then the dimensionless form can be stated as follows:

$$\frac{du}{dt} = y,$$
$$\frac{dy}{dt} = -\frac{\gamma\tau}{3m+4m_p}y - \frac{k\tau^2}{3m+4m_p}u - \frac{(m+m_p)\tau^2 F_m(t)}{(3m+4m_p)d} - V\frac{\alpha\tau^2 V_0}{(3m+4m_p)d}, \quad (6)$$
$$\frac{dV}{dt} = \frac{\alpha d}{CV_0}\frac{du}{dt} - \frac{\tau V}{V_0 CR_L}$$

Note that the position difference d transfers the coordinate system into the equilibrium point, since the amplitude of the pendulum is represented by x.

In order to perform the averaged power output as a theoretical assumption, Eq. (3) is considered in frequency domain. While the second equation in Eq. (3) is written as:

$$V = \frac{jR_L\alpha\omega_m u}{1 + jCR_L\omega_m}, \quad (7)$$

the first equation of Eq. (3) yields to:

$$V = \frac{uR_L\alpha j\omega_m\{(m+m_p)\omega_m^2 - F_0 < I_c^2 > + F_1 < I_c >\}}{(-\gamma j\omega_m - m_p\omega_m^2 - k)(1 + R_L Cj\omega_m) - \alpha^2 R_L j\omega_m} + \text{h.o.t.}, \quad (8)$$

following an arithmetic manipulation, since the harvester is driven by the field frequency ω_m. We consider that the frequency domain solutions include ω_m. Note that we consider the linear terms of the piezoelectric amplitude u in order to have an expression on power by using the above equations.

Here $<I_c>$ and $<I_c{}^2>$ indicates the time-averaged values of Eq. (5) as indicated below:

$$< I_c >= \frac{V_c}{2R_c} + \frac{V_c L\omega_m}{2\pi R_c^2}\left(2e^{-R_c\pi/L\omega_m} - 1 - e^{-R_c 2\pi/L\omega_m}\right),$$
$$< I_c^2 >= \frac{V_c^2}{2R_c^2} + \frac{V_c^2 L\omega_m}{4\pi R_c^3}\left(1 - e^{-R_c 4\pi/L\omega_m}\right) + \frac{L\omega_m}{\pi R_c}\left(e^{-R_c\pi/L\omega_m} - 1\right), \quad (9)$$

after the time integration during a certain period. Note that the electrical parameters above belong to the electromagnet coil while a certain voltage V_c with an excitation frequency of $\omega_m = 2\pi f$ is applied to the coil. In that case, one can arrive at the power relation as follows:

$$< P >= \frac{u^2 R_L\alpha^2\omega_m^2\{(m+m_p)\omega_m^2 - F_0 < I_c^2 > + F_1 < I_c >\}^2}{k^2(1+C^2R_L^2\omega_m^2) + 2k\omega_m^2(m_p + \alpha^2 CR_L^2 + C^2 m_p R_L^2\omega_m^2) + \omega_m^2\{2\alpha^2\gamma R_L + \alpha^4 R_L^2 + 2\alpha^2 Cm_p R_L^2\omega_m^2 + \gamma^2(1+C^2R_L^2\omega_m^2) + m_p^2\omega_m^2(1+C^2R_L^2\omega_m^2)\}} \quad (10)$$

While using the linear part of Eq. (8) w.r.t. u and its complex conjugate divided by load resistance R_L (i.e. $< P >=< VV^* > /R_L$), Eq. (10) gives a complete relation between the output power and both the electrical and mechanical parameters of the system. By using this equation, it is also possible to find out the optimal load resistance. If one gets the derivative of this equation w.r.t R_L, the optimal load resistance is found to be $(\omega C)^{-1}$. Here ω gives the frequency of magnetic flux and C is the capacitance of the piezoelectric layer, respectively.

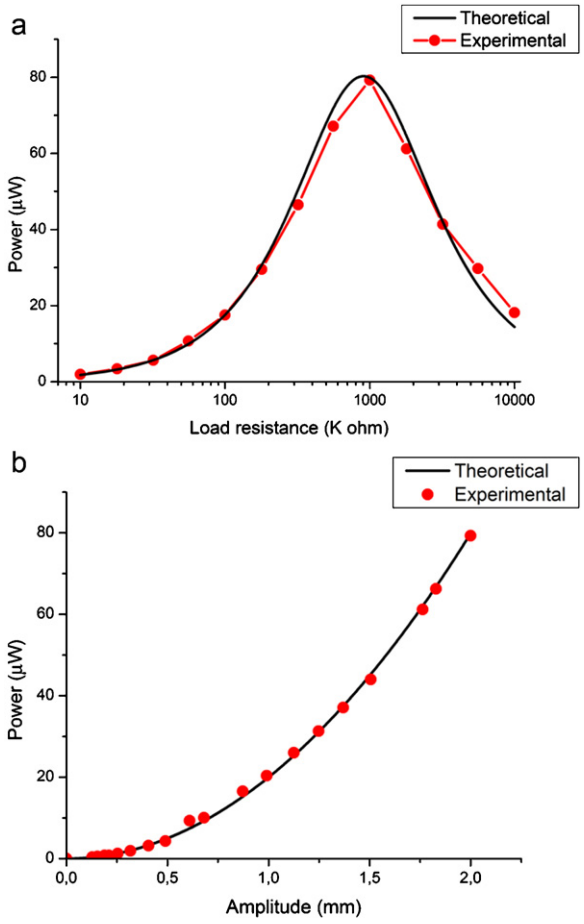

Fig. 8. The experimental and theoretical output powers as functions of load resistance (a) and PZT tip amplitude u (b). The load across the PZT is adjusted as 1 MΩ for (b). The distance d from the equilibrium point to the tip of electromagnet is 2 cm and the voltage over the electromagnet is 8 V.

In order to prove the consistence of the theoretical model with the experimental real data, the power generations as functions of R_L and the PZT tip amplitude u, are shown in Fig. 8. Note that the theoretical results in the plots have been obtained from Eq. (10). In this equation, the amplitude of piezoelastic layer $u = 2$ mm, the force/voltage ratio $\alpha = 0.0001$ N/V, $\omega_m = 4.76$ Hz, pendulum mass $m = 27.4$ g, piezoelastic layer mass $m_p = 10$ g, magnetic force coefficients $F_0 = 2750$, and $F_1 = 1500$, elastic stiffness coefficient $k = 33.435$ N/m, piezoelastic layer capacitance $C = 232$ nF, damping ratio $\gamma = 1.48$, inductance of electromagnet coil $L = 125$ mH and resistance of electromagnet coil $R_c = 5.9\,\Omega$ are used, respectively. Fig. 8(a) proves that the optimal power is obtained for a specific load resistance $R_L = 1\,\text{M}\Omega$ in both theory and experiment. Above and below of this load, the output power substantially decreases.

In the case of the amplitude (i.e. the deflection of the PZT tip), the optimal output power increases parabolic when the amplitude increases further especially for high deflections. Besides, power increases linearly at small amplitudes (i.e. for smaller amplitudes than $u = 0.5$ mm). Note also the perfect agreement between the theoretical and experimental plots.

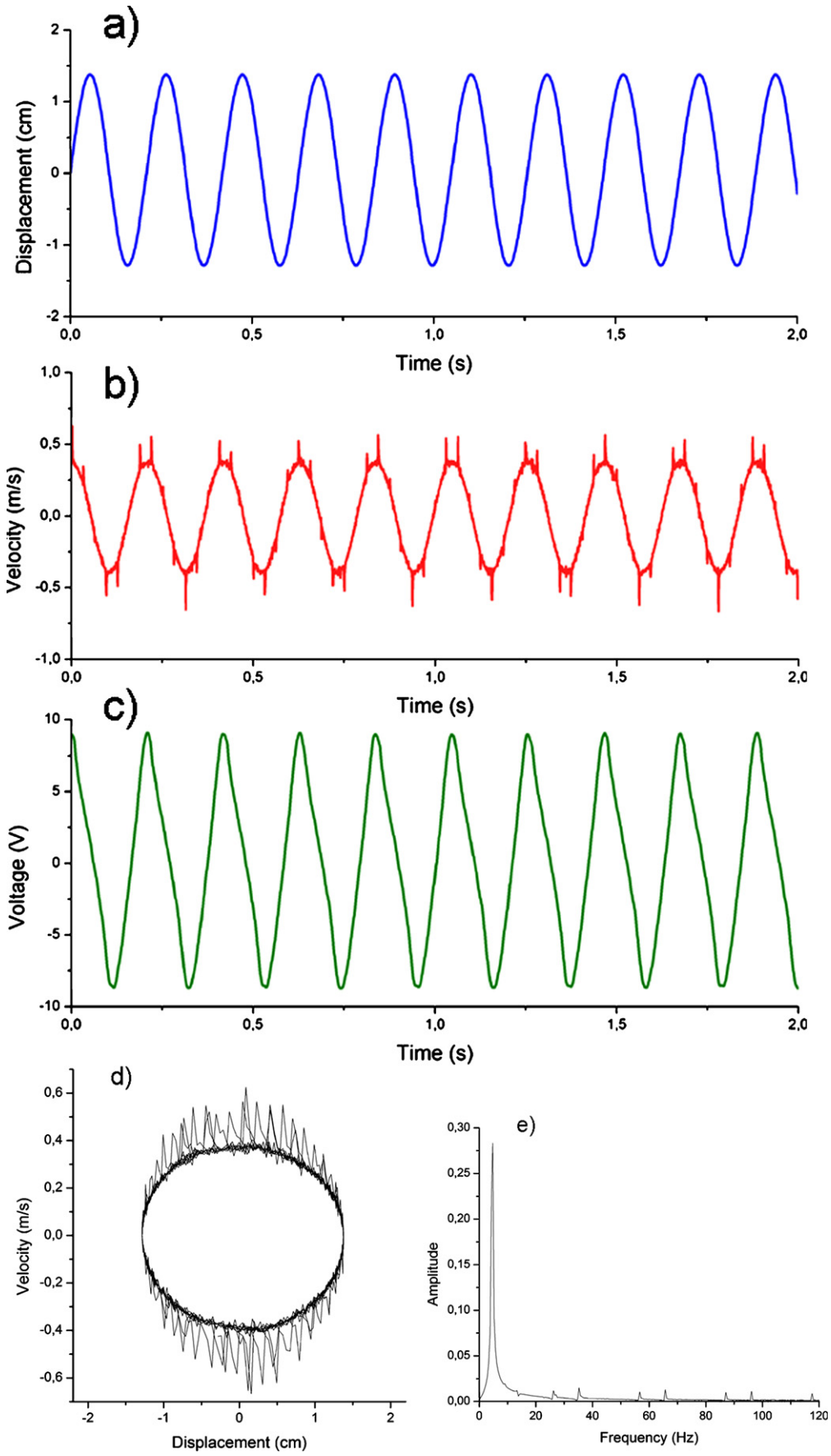

Fig. 9. The experimental results of (a) harvester tip displacement, (b) tip velocity, (c) voltage, (d) phase space portrait and (e) power spectrum of the velocity in the case $d = 2$ cm, $\omega_m = 4.76$ Hz, $R_L = 500\,\text{k}\Omega$.

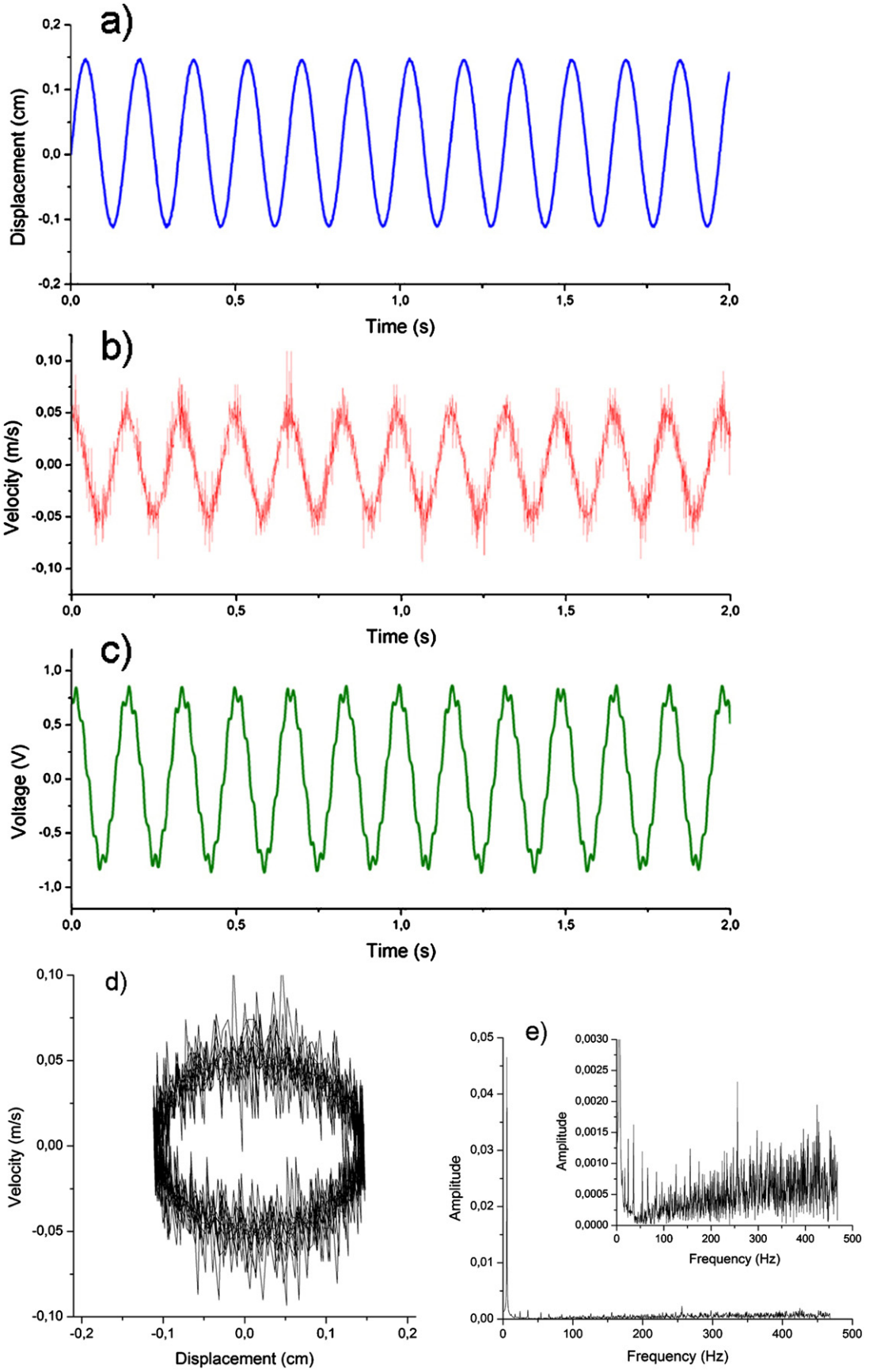

Fig. 10. The experimental results of (a) harvester tip displacement, (b) tip velocity, (c) voltage, (d) phase space portrait and (e) power spectrum of the velocity in the case $d = 2$ cm, $\omega_m = 6.09$ Hz, $R_L = 500$ kΩ.

4. Results and discussion

In this section, the experimental results with regard to displacement (i.e. the harvester amplitude), velocity and voltage will be discussed. In this manner, we start with Fig. 9, where the natural frequency of the harvester equals to the magnetic field excitation frequency $\omega_m = 4.76$ Hz. While the tip mass displacement produces a sinusoidal function, it slightly deviates from the ideal sinusoidal function, when the displacement variation becomes maximal. This is proven by an intuitive plot of tip mass velocity. Note that the ripples around the minimal and maximal parts of velocity data survive for the entire data set. Therefore we have sketched out phase space portrait in order to explore this situation. As one can see in the last plot, the ripples destroy the ideal elliptic trajectory. Although an ideal periodic motion yields to a simple circle or ellipse in the phase space, the ripples here point out a non-regular dynamics even at the natural frequency of the system. Another point on this response is that these ripples cannot be related to any noise phenomena since the external magnetic excitation is very strong for the adjusted parameter set. Strictly speaking, the current flowing in the electromagnet coil has the maximal value of $I_c = 1.3$ A, which generates magnetic force at the core tip of the electromagnet and a flux density of 102 G has been measured 2 cm away from the core tip by a FW-Bell 5170 type gaussmeter.

According to the power spectrum of the velocity data, there exist different high frequency components which prove the existence of the ripples at the minimal and maximal amplitudes of the velocity data. Strictly speaking, the main frequency 4.7 Hz and other high frequency components (14.6 Hz, 26.3 Hz, 34.9 Hz, 56.3 Hz, etc.) are clearly seen in the spectrum.

When the excitation frequency ω_m changes from the natural frequency to 6.09 Hz, the scenario becomes much complicated (Fig. 10). Beside the main frequency of 6.09 Hz, there exist infinite numbers of frequencies in the spectrum as shown the inset of Fig. 10(e). Some frequencies with larger amplitudes can be summarized as follows: 24 Hz, 36 Hz, 54 Hz, 156 Hz, 256 Hz, 425 Hz, 452 Hz etc.. . . The frequency diversity can also be observed in velocity values in Fig. 10 as infinite numbers of ripples. The ripples in velocity are reflected to the experimental voltage values in Fig. 10(c), therefore these ripples are important for such harvesting systems under a changeable magnetic excitation. Strictly speaking, the pendulum has its natural frequency ω_0 and as an external effect – excitation frequency of the field ω_m also contributes to its dynamics. This combination of the frequencies can exert some higher modes and their amplitudes increase substantially in the spectra. Even at the situation $\omega_m = \omega_0$, there exist certain higher frequencies appearing at the spectra. However if the field frequency changes to another value different than ω_0, some other higher frequencies of cantilever modes are excited substantially as a result of frequency combination. Thus, one can observe a wider spectrum. Therefore it is obvious that magnetic force excites the cantilever modes with regard to the excitation frequency and causes wider spectra with high harmonics. Since we have strong field strength in two cases (with high and low frequencies), we must say that they are not noise but the combined effect of field frequency and natural frequency. We can prove it with one of our recent study [5] that theoretical solution of the system of equations produces same ripples at the velocity data. On the other hand, the ripples also do not come from the mechanical noise, in fact the magnetic flux is still strong with the same winding current in the electromagnet as in Fig. 9. Therefore these ripples are considered as the characteristic feature for such excited systems. On the other hand, high frequency components of the spectrum such as 425 Hz and 452 Hz are observed first time, experimentally in such a large-scale piezoelectric system to our knowledge. This phenomenon encourages us to obtain better power solutions for magnetically excited media at inconstant

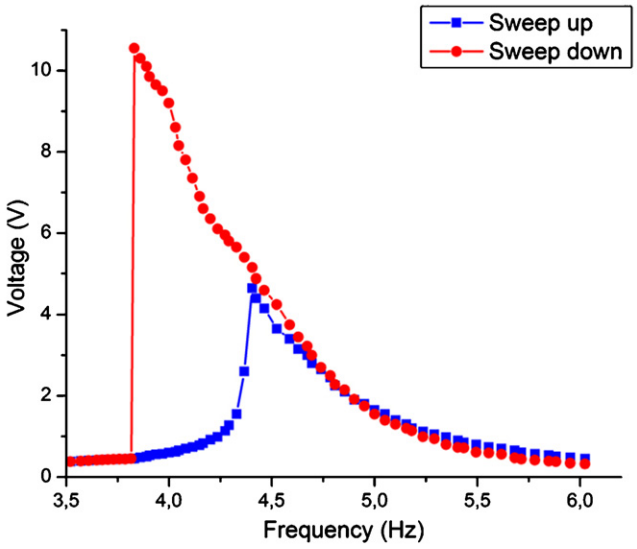

Fig. 11. Peak voltage as function of the excitation frequency ω_m. Softening effect is observed for the sweep up/down cases. The parameters are $d = 2$ cm, the load resistance $R_L = 820$ kΩ and the square voltage over electromagnet $V_c = 8$ V.

excitation frequencies. Although the displacement appears sinusoidal, the wide-band structure in velocity causes smooth power decay for different excitation frequencies as will be shown in Fig. 12(a) and (b). Due to the periodic magnetic force which has different excitation frequencies than the natural one, a wide-band velocity spectra is observed. This proves that periodic magnetic excitation produces a wide-band velocity spectra and this yield to much complicated voltage signals with other frequencies as in Fig. 10(c).

Fig. 11 shows the softening effect of the magnetic field frequency ω_m. Softening effect in a piezoelectric material is caused by the nonlinear elasticity of piezoelectric material [23]. When the amplitude of piezoelectric pendulum increases, the piezoelectric material shows an elastic force as function of cubic order of amplitude in addition to the linear one. Moreover, more flexible materials demonstrate not only increased softening effects, but also intrinsic features of the material play an important role as well [24]. On the other hand, magnetic excitation term F_m (see in Eq. (5)) includes the cubic nonlinearities. When the pendulum oscillates at higher frequencies on the sweep-down line as in Fig. 11, amplitude increases drastically at lower frequencies. However, when it starts to oscillate at lower frequencies on the sweep-up line, amplitude reaches upto a lower amplitude compared to earlier case, and starts to decrease again. Since F_m in Eq. (5) is found as cubic function of amplitude (i.e. u), amplitude increment from the equilibrium point of pendulum does not yield to higher elastic force due to the second-order term in u. This feature enforces the system to behave in softening manner. For the dynamic analogy of the piezoelectric hardening/softening effect, we refer to Ref [25,26] in order to explain this effect in terms of nonlinearity.

It is obvious that the generated voltage strictly depends on the excitation frequency. While ω_m decreases from its high value (i.e. 6 Hz), voltage values increase upto 11 V; however if one sweeps up excitation frequency ω, voltage initially increases smooth till one reaches $\omega_m = 4.25$ Hz, then a jump to 5 V is observed and the curve starts to decrease for high excitation frequencies. To our knowledge, it is the first time that the magnetic frequency sweeping yields to a softening effect. While the softening effect causes a hysteresis loop at the left-hand side of the natural frequency, the hardening effect causes a hysteresis loop at the right-hand side for different excitation systems [26,27]. When the excitation frequency comes

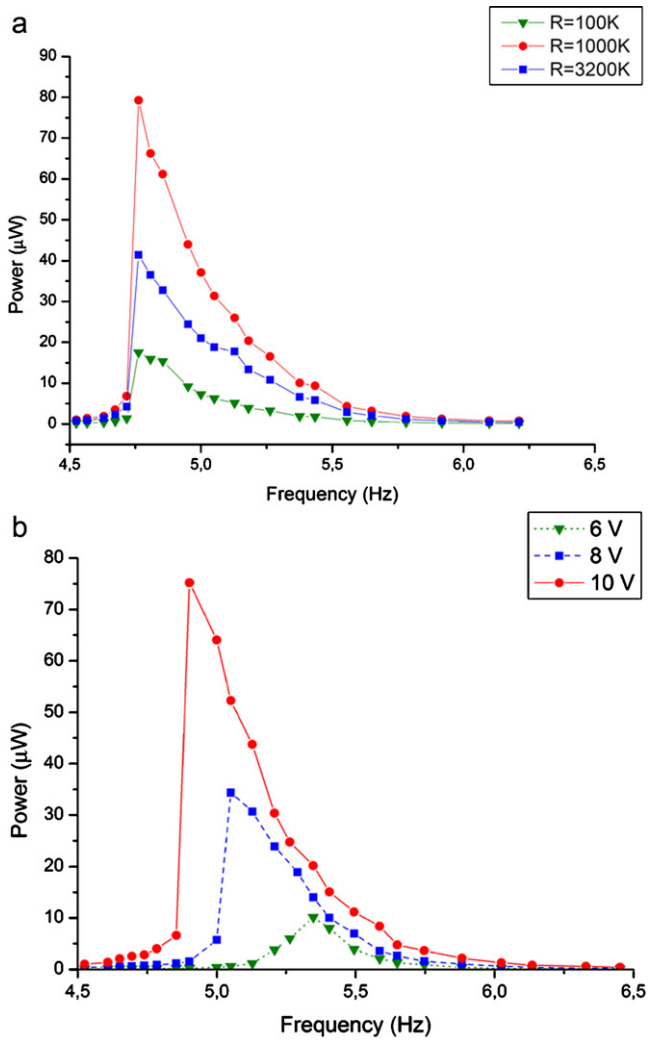

Fig. 12. (a) Generated power as function of frequency in the case of different resistive loads. The parameters are $d = 2$ cm and the square voltage over electromagnet $V_c = 8$ V. (b) The averaged power as function of frequency in the cases of different magnetic forces at $d = 2.6$ cm and $R_L = 820$ KΩ. Both figures have been obtained in sweep-up case.

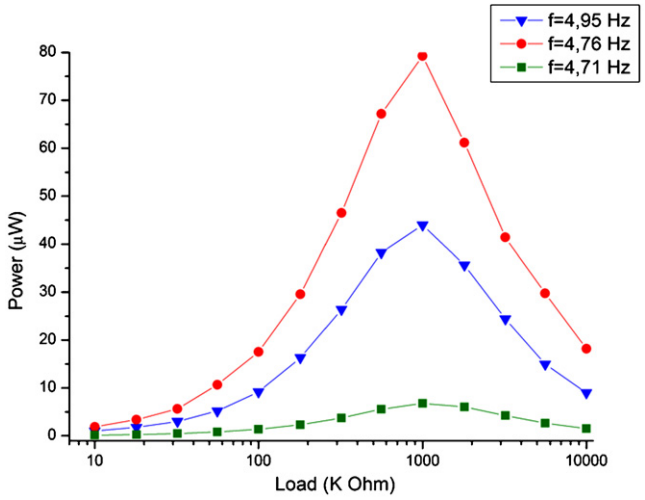

Fig. 13. Generated power as function of resistive loads in the case of different excitation frequencies. The parameters are $d = 2$ cm and the square voltage over electromagnet $V_c = 8$ V.

closer to the natural frequency in sweeping-up case, the oscillations become dominant and the peak voltage values increase drastically. For instance, if one considers using such a harvester in a magnetic media produced by a source, the natural frequency of the harvester beam should be close to that frequency for the most efficient voltage output. Note also that the frequency adjustment can be applied from the high frequency value, if higher voltage amplitudes are desired in that system.

The averaged output power of the PZT harvester can be defined as follows from the experimental data according to the formulation $<P> = <V^2>/R_L$ as also pointed out in the previous section.

In order to determine the averaged power of the energy harvester, we have explored the frequency dependence at different loads (Fig. 12(a)). Strictly speaking, the characteristics of the voltage outputs in Fig. 10 are also obvious in this plot. The output power is low for relatively smaller frequencies than the natural one. A maximal output power is obtained when the natural frequency is applied to the harvester as the excitation frequency. On the other hand, the load plays an important role to gain the maximal output power from the harvester as we have claimed in the earlier section. According to the detailed analyses, the load of 1 MΩ receives the maximal power from the system due to the fact that the internal impedance of the harvesting system exists around that value. The effect of magnetic force upon the harvester can be seen clearly in Fig. 12(b). When the magnetic force increases, the maximal averaged power is obtained at lower frequencies. In other words, if the excitation force increases, the maximal power is obtained around the natural frequency ω_0. This reality enforces us to consider the wide-band frequency response in velocity data as in Fig. 10(e). Thus, this velocity data affects the voltage output is taken at different frequencies ω_m than the natural one ω_0. This phenomenon is observed for the first time under a changeable magnetic field to our knowledge. In addition, Fig. 12(b) proves that the magnetic force increment yields to higher powers for wide ranges of frequencies. For instance, the coil voltage $V_c = 10$ V gives at least 30 μW between $\omega_m = 4.8$ Hz and $\omega_m = 5.2$ Hz. When the magnetic force is decreased, the frequency ranges where high powers are observed become narrow.

Fig. 13 shows the variation of the averaged power of the harvester system as function of the load. This graph shows that a maximal power output can be obtained in terms of resistive loads. In addition, the effect of the excitation frequency should also be underlined for the maximal power generation. Note that the natural frequency of the system is $\omega_m = 4.76$ Hz for these measurements. If we consider the results of a different experimental harvesting system, which is proposed by Cottone et al. [7], their maximal averaged power is around 3 μW. Their inverted pendulum in a noisy magnetic field produced by two coils can produce less power compared to our results. Therefore we believe that our energy harvesting system is more efficient under low frequency magnetic excitations.

A much intuitive 3D power graph is shown in Fig. 14. There exists a certain maximum for specific resistance and magnetic excitation frequency. Note that the output power of PZT harvester becomes maximal when the excitation frequency gets closer to the natural frequency of the harvester. While the dependence on the frequency is much strict in order to get the maximal output, the resistance dependence affects the output power relatively low. Note that the resistance axis is in the logarithmic scale. Another important result is that the harvester power shows the wider frequency region at its same value for the resistive loads of 1 MΩ. Thus if one requires much stable output for a wider range of excitation frequencies from the harvester, the load should be adjusted at that value otherwise the maximal output can be generated at certain parameters.

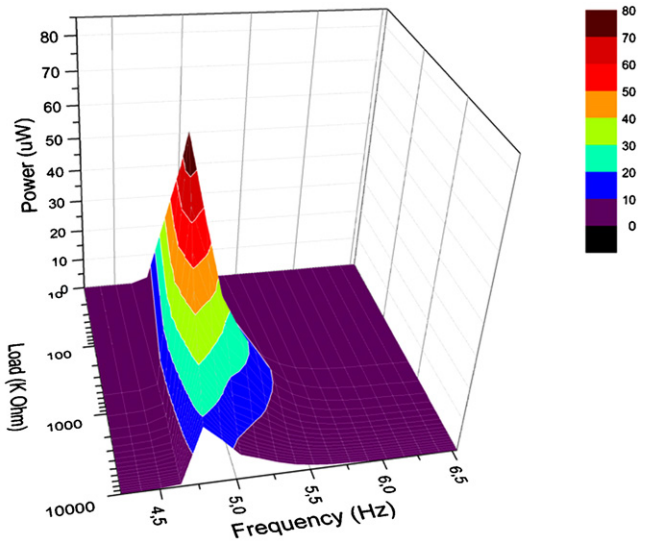

Fig. 14. Generated power on the plane of resistive load and excitation frequency ω_m. The parameters are $d = 2$ cm and the square voltage over electromagnet $V_c = 8$ V.

5. Conclusion

The influence of periodic magnetic excitation to a harvester has been explored. The amplitude of the voltage increases linearly by the position to the equilibrium point of the pendulum at the operation region. The power dependencies on load and the magnetic excitation frequency are clarified, experimentally and theoretically. Theoretical and experimental results are found to be consistent with each other. Simulation studies prove that the magnetic force includes the terms of current inside the electromagnet windings and the position to the electromagnet. Although the nonlinear terms of displacement is neglected, the theoretical power output agrees very well with the experiments. The magnetic excitation frequency and field force become vital in order to obtain the maximal power. According to our experimental results, the proposed harvester generates much power compared to the other proposed harvesters which operate under the random magnetic field. The periodic field excitation causes ripples at the velocity of harvester tip and that yields to wide-band frequency behavior. By changing the magnetic force strength, both the maximal voltage and power skip to lower frequencies. Therefore an effective softening effect is observed for periodic field excitation. This new harvester can be attached anywhere having a changeable magnetic flux such as motors, generators other magnetic rotating devices for an alternative energy harvesting mechanism.

Acknowledgements

The authors acknowledge the support of Gazi University – Scientific Research Project Unit under the Project no. BAP 07/2010-01 and the support of TUBITAK Graduate School Programme ISMFA 2011 under no: 2217.

References

[1] M. Ferrari, V. Ferrari, M. Guizzettia, B. Andò, S. Baglio, C. Trigona, Improved energy harvesting from wideband vibrations by nonlinear piezoelectric converters, Sensors and Actuators A 162 (2010) 425–431.
[2] K.A. Cook-Chennault, N. Thambi, A.M. Sastry, Powering MEMS portable devices-a review of non-regenerative and regenerative power supply systems with special emphasis on piezoelectric energy harvesting systems, Smart Materials and Structures 17 (2008) 1–33.
[3] P.D. Mitcheson, E.M. Yeatman, G.K. Rao, A.S. Holmes, T.C. Green, Energy harvesting from human and machine motion for wireless electronic devices, Proceedings of IEEE 96 (2008) 1454–1486.
[4] E.P. James, M.J. Tudor, S.P. Beeby, N.R. Harris, P. Glynne-Jones, J.N. Ross, N.M. White, An investigation of self-powered systems for condition monitoring applications, Sensors and Actuators A 110 (2004) 171–176.
[5] Y. Uzun, E. Kurt, Implementation and modeling of a piezoelastic pendulum under a harmonic magnetic excitation, in: 11th International Conference on Applications of Electrical Engineering, Athens, Greece, 2012.
[6] L. Mateu, F. Moll, Review of energy harvesting techniques and applications for microelectronics, in: Proceedings of the SPIE Microtechnologies for the New Millenium, 2005, pp. 359–373.
[7] F. Cottone, H. Vocca, L. Gammaitoni, Nonlinear energy harvesting, Physical Review Letters 102 (2009) 080601-1–080601-4.
[8] D. Zhu, M.J. Tudor, S.P. Beeby, Strategies for increasing the operating frequency range of vibration energy harvesters: a review, Measurement Science and Technology 21 (2010) 1–29.
[9] S.C. Stanton, C.C. McGehee, B.P. Mann, Nonlinear dynamics for broadband energy harvesting: investigation of a bistable piezoelectric inertial generator, Physica D 239 (2010) 640–653.
[10] J. Qiu, J.H. Lang, A.H. Slocum, A curved-beam bistable mechanism, IEEE ASME Journal of Microelectromechanical Systems 13 (2004) 137–146.
[11] R. Ramlan, M.J. Brennan, B.R. Mace, I. Kovacic, Potential benefits of a nonlinear stiffness in an energy harvesting device, Nonlinear Dynamics 59 (2010) 545–558.
[12] E. Kurt, R. Kasap, S. Acar, Effects of periodic magnetic field to the dynamics of vibrating beam, Mathematical and Computational Applications Journal 9 (2004) 275–284.
[13] E. Kurt, Nonlinear responses of a magnetoelastic beam in a step-pulsed magnetic field, Nonlinear Dynamics 45 (2006) 171–182.
[14] S.M. Shahruz, Increasing the efficiency of energy scavengers by magnets, Journal of Computational and Nonlinear Dynamics 3 (2008) 041001-1–041001-12.
[15] J.T. Lin, B. Lee, B. Alphenaar, The magnetic coupling of a piezoelectric cantilever for enhanced energy harvesting efficiency, Smart Materials and Structures 19 (2010) 1–7.
[16] S. Roundy, P.K. Wright, A piezoelectric vibration based generator for wireless electronics, Smart Materials and Structures 13 (2004) 1131–1142.
[17] L. Wang, F.G. Yuan, Vibration energy harvesting by magnetostrictive material, Smart Materials and Structures 17 (2008) 045009-1–045009-14.
[18] Y. Uzun, E. Kurt, Energy harvesting from the varying magnetic field of an operating induction motor, in: 3. Int. Conf. on Nuclear and Renewable Energy Resources, Istanbul, Turkey, 2012.
[19] A. Borin, L., Girometta, G. Venchi, Development of a leakage flux measurement system for condition monitoring of electrical drives, 2011 IEEE International Symposium on Diagnostics for Electric Machines, Power Electronics & Drives, Bologna, 2011.
[20] V.R. Challa, M.G. Prasad, F.T. Fisher, A coupled piezoelectric–electromagnetic energy harvesting technique for achieving increased power output through damping matching, Smart Materials and Structures 18 (2009) 095029-1–095029-11.
[21] G.K. Ottman, H.F. Hofmann, A.C. Bhatt, G.A. Lesieutre, Adaptive piezoelectric energy harvesting circuit for wireless remote power supply, IEEE Transactions on Power Electronics 17 (2002) 669–676.
[22] J.H. Cho, R.F. Richards, D.F. Bahr, C.D. Richardsa, Efficiency of energy conversion by piezoelectrics, Applied Physics Letters 89 (2006) 104107-1–104107-3.
[23] S.C. Stanton, A. Erturk, B.P. Mann, E.H. Dowell, D.J. Inman, Nonlinear nonconservative behavior and modeling of piezoelectric energy harvesters including proof mass effects, Journal of Intelligent Material Systems and Structures 23 (2) (2012) 183–199.
[24] S.C. Stanton, A. Erturk, B.P. Mann, D.J. Inman, Resonant manifestation of intrinsic nonlinearity within electroelastic micropower generators, Applied Physics Letters 97 (2010) 254101-1–254101-3.
[25] D.S. Nguyen, E. Halvorsen, Analysis of vibration energy harvesters utilizing a variety of nonlinear springs, in: PowerMEMS 2010 Conference, Leuven, Belgium, 2010.
[26] S.C. Stanton, C.C. McGehee, B.P. Mann, Reversible hysteresis for broadband magnetopiezoelastic energy harvesting, Applied Physics Letters 95 (2009) 174103-1–174103-3.
[27] E. Sardini, M. Serpelloni, An efficient electromagnetic power harvesting device for low-frequency applications, Sensors and Actuators A 172 (2011) 475–482.

Biographies

Yunus Uzun, born in Kayseri Turkey in 1979. He received his B.S., M.Sc. and Ph.D. degrees from the Gazi University in 2000, 2004 and 2012, respectively. He worked as a high school teacher on electrics from his graduation to 2008. He has been a lecturer in the Department of Electrics and Energy of Ahi Evran University for 4 years. His main research area focuses on the experimental and theoretical explorations of energy harvesting systems.

Erol Kurt, born in Unye Turkey completed his undergraduate degree at Gazi University, Department of Physical Education in 1998 and took his M.Sc. degree from the Institute of Science & Technology of the same university in 2001. He was awarded by an European Graduate College Grant during his Ph. D study at the Institute of Physics & Mathematics of Bayreuth University (Germany). He completed his Ph. D. degree in 2004 on the instabilities of rotating magnetic fluids there. Then he worked in Turkish Atomic Energy Authority R&D Department, Fusion Division for 3 years.

Beginning from the middle of 2009, he was assigned to the position of Associate Professor at Technology Faculty of Gazi University in Ankara. His main teaching and research areas include nonlinear phenomena in electrical/electronic circuits, electric machine design, mechanical vibrations, chaos, plasmas, fusion and magnetohydrodynamics. He has authored or co-authored many scientific papers and organized serial conferences of Int. Conf. Nuclear & Renewable Energy Resources (NuRER) and European Workshop on Renewable Energy Systems (EWRES). He has carried out the guest editorship of several special issue journals, the editorship of TUBAV Journal of Science from September 2011 and the membership of the editorial board of Sci. J. Circuits, Sys. Signal Processing.